Self-interacting dark matter model without dark energy in cosmology

Yixuan Zhu[1]

[1]*Department of Astronomy, Beijing Normal University. Beijing 100875. PR China*

ABSTRACT

1. INTRODUCTION

2. THE BASIC EQUATIONS IN THE IDM MODEL

We assume that the total density of the cosmic fluid obeys the collisional Boltzmann equation

$$\dot{\rho} + 3H\rho + \kappa\rho^2 - 2\Psi = 0, \tag{1}$$

where ρ is the total energy-density of the cosmic fluid, containing dark matter, baryons, and any type of exotic energy, Ψ is the rate of creation of DM particle pairs, and the annihilation parameter $\kappa(\geq 0)$ is given by:

$$\kappa = \frac{\langle \sigma u \rangle}{M_x}, \tag{2}$$

where σ is the cross-section for annihilation, u is the mean particle velocity, and M_x is the mass of the DM particle. Compared to the usual fluid equation, the effective pressure term is

$$P = \frac{\kappa\rho^2 - \Psi}{3H}. \tag{3}$$

When $\kappa\rho^2 - \Psi < 0$, what means that the IDM particle creation term is larger than the annihilation item, IDM may serve as a negative pressure source in the global dynamics of the Universe, like the role of Dark Energy in the general cosmological models.

Basilakos & Plionis (2009) identified two functional forms for which the previous Boltzmann equation can be solved analytically. Refering to Appendix B in Basilakos & Plionis (2009), only one of these two is of interest because it provides a "$\propto a^{-3}$" dependence of the scale factor, which is

$$\Psi(a) = aH(a)R(a) = C_1(n+3)a^n H(a) + \kappa C_1^2 a^{2m}. \tag{4}$$

And the total energy density is

$$\rho(a) = C_1 a^n + \frac{a^{-3}F(a)}{C_2 - \int_1^a x^{-3}f(x)F(x)\mathrm{d}x}, \tag{5}$$

where $f(a) = -\kappa/[aH(a)]$, and the kernal function $F(a)$ has the form

$$F(a) = \exp\left[-2\kappa C_1 \int_1^a \frac{x^{n-1}}{H(x)}\mathrm{d}x\right]. \tag{6}$$

The first term of Eq.(5) is the density corresponding to the residual matter creation that results from a possible disequilibrium between the particle creation and annihilation processes, while the second term can be viewed as the energy density of the self-IDM particles that are dominated by the annihilation process.

2.1. *Model 1: relation to the ΛCDM model*

If $n = 0$, the global density evolution can be transformed as

$$\rho(a) = C_1 + a^{-3}\frac{e^{-2\kappa C_1(t-t_0)}}{C_2 - \kappa Z(t)}, \tag{7}$$

where $Z(t) = \int_{t_0}^t a^{-3}e^{-2\kappa C_1(t'-t_0)}\mathrm{d}t'$(Basilakos & Plionis (2009)). Using the usual unit-less Ω-like parameterization, we obtain that

$$\left(\frac{H}{H_0}\right)^2 = \Omega_{1,0} + \frac{\Omega_{1,0}\Omega_{2,0}a^{-3}e^{-2\kappa C_1(t-t_0)}}{\Omega_{1,0} + \kappa C_1\Omega_{2,0}Z(t)}, \tag{8}$$

where $\Omega_{1,0} = 8\pi G C_1/3H_0^2$ and $\Omega_{2,0} = 8\pi G/3H_0^2 C_2$, which related to Ω_Λ and Ω_m in the ΛCDM model, respectively. From Eq.(2), we can also give the mass of the DM particle related to the range of κC_1(in the unit of Gyr^{-1})

$$M_x = \frac{3.325 \times 10^{-12}}{\kappa C_1}\frac{\langle \sigma u \rangle}{10^{-23}}h^2(1 - \Omega_{2,0})\,\mathrm{GeV}, \tag{9}$$

where $h \equiv H_0/[100\mathrm{km/s/Mpc}]$.

2.2. *Model 2 : relation to the wCDM model*

If $\kappa = 0$, the global density evolution can be written as

$$\rho(a) = \mathcal{D}a^{-3} + C_1 a^n, \tag{10}$$

where $\mathcal{D} = C_2 - C - 1$. The conditions in which the current model acts as a quintessence cosmology are given by $\mathcal{D} > 0, C_1 > 0$, and $w_{\mathrm{IDM}} = -1 - n/3$. This solution is mathematically equivalent to that of the gravitational matter creation model of(). The Hubble flow is now given by

$$\left(\frac{H}{H_0}\right)^2 = \Omega_{2,0}a^{-3} + \Omega_{1,0}a^n, \tag{11}$$

where $\Omega_{2,0} = 8\pi G\mathcal{D}/3H_0^2$ and $\Omega_{1,0} = 8\pi G C_1/3H_0^2$, respectively.(Basilakos & Plionis (2009))

3. DATASET

To constrain the relevant IDM models (Basilakos & Plionis (2009)), we use the newly revised observational $H(z)$ data (OHD)(Simon et al. (2005); Stern et al. (2010);Moresco et al. (2012);Zhang et al. (2014); Moresco et al. (2016);Ratsimbazafy et al. (2017);Moresco (2015); Borghi et al. (2022);Jiao et al. (2023)),the Pantheon+ set of 1701 SNe Ia (Scolnic et al. (2022)), the QSO data from Lusso, E. et al. (2020), the BAO data from SDSS and DESI 2024.

3.1. *The observational H(z) data*

It is widely known that the Hubble parameter $H(z)$ depends on the differential age as a function of redshift z in the form

$$H(z) = -\frac{1}{1+z}\frac{\mathrm{d}z}{\mathrm{d}t}, \tag{12}$$

which provides a direct measurement on $H(z)$ based on $\mathrm{d}z/\mathrm{d}t$. OHD measurements have recently been acquired mainly employing cosmic chronometers (CC). The CC method is used to provide 33 observational data points, which are taken in the redshift range [0.07, 1.965]. The Table 1 lists the OHD dataset used in this analysis. In this case, χ^2 can be defined as

$$\chi^2_{\mathrm{OHD}} = \sum_i^{33} \frac{(H_{\mathrm{th}} - H_{\mathrm{data}})^2}{\sigma_i^2}. \tag{13}$$

3.2. *Type Ia supernovae*

SNe Ia have long been used as "standard candles" to give a direct measurement of their luminosity distance, and provides strong constraints on cosmological parameters. We use the latest Pantheon+ data set of 1701 SNe Ia samples(Scolnic et al. (2022)), which covers the redshift range [0, 2.26].

We use the fiducial SN Ia magnitude (M_b) determined from SH0ES 2021 Cepheid host distances(Riess et al. (2022)), which gives the μ_{data} and we give the χ^2 as

$$\chi^2_{\mathrm{SNe}} = \Delta^{\mathrm{T}} C^{-1} \Delta, \tag{14}$$

where $\Delta = (\mu_{\mathrm{th}} - \mu_{\mathrm{data}})$ and C^{-1} is the inverse of the covariance matrix of the SNe Ia data, the distance modulus is $\mu = 5\log_{10}(d_L/\mathrm{Mpc}) + 25$, and the luminosity distance d_L can be given as a function of redshift z

$$d_L = (1+z)\int_0^z \frac{\mathrm{c}\mathrm{d}z'}{H(z')}. \tag{15}$$

To eliminate the advanced restriction to H_0 from M_b, we adopt the likelihood function as

$$\widetilde{\chi}^2_{\mathrm{SNe}} = \chi^2_{\mathrm{SNe}} - \frac{B^2}{C} + \ln\left(\frac{C}{2\pi}\right), \tag{16}$$

Table 1. The OHD dataset

z	$H(z)$	Reference
0.07	69±19.6	Zhang et al. (2014)
0.09	69±12	Simon et al. (2005)
0.12	68.6±26.2	Zhang et al. (2014)
0.17	83±8	Simon et al. (2005)
0.179	75±4	Moresco et al. (2012)
0.199	75±5	Moresco et al. (2012)
0.2	72.9±29.6	Zhang et al. (2014)
0.27	77±14	Simon et al. (2005)
0.28	88.8±36.6	Zhang et al. (2014)
0.352	83±14	Moresco et al. (2012)
0.3802	83±13.5	Moresco et al. (2016)
0.4	95±17	Simon et al. (2005)
0.4004	77±10.2	Moresco et al. (2016)
0.4247	87.1±11.2	Moresco et al. (2016)
0.4497	92.8±12.9	Moresco et al. (2016)
0.47	89±34	Ratsimbazafy et al. (2017)
0.4783	80.9±9	Moresco et al. (2016)
0.48	97±62	Stern et al. (2010)
0.593	104±13	Moresco et al. (2012)
0.68	92±8	Moresco et al. (2012)
0.75	98.8±33.6	Borghi et al. (2022)
0.781	105±12	Moresco et al. (2012)
0.8	113.1±15.1	Jiao et al. (2023)
0.875	125±17	Moresco et al. (2012)
0.88	90±40	Stern et al. (2010)
0.9	117±23	Simon et al. (2005)
1.037	154±20	Moresco et al. (2012)
1.3	168±17	Simon et al. (2005)
1.363	160±33.6	Moresco (2015)
1.43	177±18	Simon et al. (2005)
1.53	140±14	Simon et al. (2005)
1.75	202±40	Simon et al. (2005)
1.965	186.5±50.4	Moresco (2015)

where $B = \Delta^{\mathrm{T}} C^{-1}$ and C is the sum of C^{-1}. Apparently these two functions give the same constraints in $\Omega_{2,0}$ and $\log_{10}(\kappa C_1)$.

3.3. *Quasar*

The quasar gives a higher redshift than SNe Ia. We use the QSO dataset from Lusso, E. et al. (2020), which gives 2421 samples with the ultraviolet (UV) and X-ray luminosity. The redshift is up to $\simeq 7.5$.

The $L_X - L_{UV}$ relation of quasar is usually written as

$$\log_{10}(L_X) = \beta + \gamma \log_{10}(L_{UV}), \tag{17}$$

which gives that

$$\log_{10}(F_X) = \beta + (\gamma - 1)\log_{10}(4\pi) + \gamma\log_{10}(F_{UV})$$
$$+ 2(\gamma - 1)\log_{10}(d_L), \qquad (18)$$

where d_L is the luminosity distance same as Eq.(15). Here we use the parameters defined in Li et al. (2024), which gives

$$\beta = \beta_0 + \beta_1(1 + z), \gamma = \gamma_0 + \gamma_1(1 + z), \qquad (19)$$

so the χ^2 function for the QSO data can be defined as

$$\chi_{\mathrm{QSO}}^2 = \sum_i^{2421}\left[\frac{(y_{\mathrm{th}}^2 - y_{\mathrm{data}}^2)}{s_i^2} - \ln(2\pi s_i^2)\right], \qquad (20)$$

where $s_i^2 = \mathrm{d}y_i^2 + \gamma^2\mathrm{d}x_i^2 + \delta^2$ refers to the uncertainties on the x_i ($\log_{10} F_X$) and y_i ($\log_{10} F_{UV}$) and δ_i represent the instrinsic dispersion.

3.4. *Baryon acoustic oscillation*

The Baryon acoustic oscillation method (BAO) provides a key cosmological probe sensitive to the cosmic expansion history with well-controlled systematics. We use two BAO data sets from the SDSS(Alam et al. (2021)) and DESI 2024(Collaboration et al. (2024)), which are given at Table 2 and Table 3, respectively. The redshift is up to 2.33 both in the SDSS and the DESI 2024 dataset.

The χ^2 function for the BAO data is defined as

$$\chi_{\mathrm{BAO}}^2 = \sum_i \frac{(D_{\mathrm{th}}/r_{\mathrm{d}} - D_{\mathrm{data}}/r_{\mathrm{d}})^2}{\sigma_i^2}, \qquad (21)$$

where D refers to D_{M}, D_{H}, or D_{V}, which ara given as

$$D_{\mathrm{M}}(z) = c\int_0^z \frac{\mathrm{d}z'}{H(z')}, \qquad (22)$$

$$D_{\mathrm{H}}(z) = \frac{c}{H(z)}, \qquad (23)$$

$$D_{\mathrm{V}}(z) = \left[zD_{\mathrm{M}}^2(z)D_{\mathrm{H}}(z)\right]^{1/3}, \qquad (24)$$

and r_{d} is the sound horizon at the drag epoch, which is given as

$$r_{\mathrm{d}} = \int_{z_{\mathrm{drag}}}^\infty \frac{c_s(z')\mathrm{d}z'}{H(z')}, \qquad (25)$$

where c_s is the sound speed prior to recombination, which is given as

$$c_s(z) = \frac{c}{\sqrt{3\left(1 + \frac{3\rho_{\mathrm{b}}(z)}{4\rho_\gamma(z)}\right)}} \simeq \frac{c}{\sqrt{3\left(1 + \frac{3\rho_{\mathrm{b}0}}{4\rho_{\gamma0}}\frac{1}{1+z}\right)}}. \qquad (26)$$

However, the solution of Eq.(8) only gives an upper limit of redshift $z_{\max}$ (see Appendix), and we just try to use the cross parameter $r_{\mathrm{d}}h$ to give the constraints.

Table 2. The BAO-only dataset from SDSS

z_{eff}	$D_{\mathrm{M}}/r_{\mathrm{d}}$	$D_{\mathrm{H}}/r_{\mathrm{d}}$	$D_{\mathrm{V}}/r_{\mathrm{d}}$
0.15			4.47±0.17
0.38	10.23±0.17	25±0.76	
0.51	13.36±0.21	22.33±0.58	
0.7	17.86±0.33	19.33±0.53	
0.85			$18.33^{+0.57}_{-0.62}$
1.48	30.69±0.8	13.26±0.55	
2.33	37.6±1.9	8.93±0.28	
2.33	37.3±1.7	9.08±0.34	

Table 3. The BAO dataset from DESI 2024

z_{eff}	$D_{\mathrm{M}}/r_{\mathrm{d}}$	$D_{\mathrm{H}}/r_{\mathrm{d}}$	$D_{\mathrm{V}}/r_{\mathrm{d}}$
0.295			7.93±0.15
0.51	13.62±0.25	20.98±0.61	
0.706	16.85±0.32	20.08±0.6	
0.93	21.71±0.28	17.88±0.35	
1.317	27.79±0.69	13.82±0.42	
1.491			26.07±0.67
2.33	39.71±0.94	8.52±0.17	

4. CONSTRAINT RESULTS

We use the Markov chain Monte Carlo (MCMC) method based on the opening package `emcee` to give a global constraints to the free parameters $\Omega_{2,0}$ and $\log_{10}(\kappa C_1)$ in Model 1 and n in Model 2. Besides, we also add the parameter H_0 or h to give the constraints to the dark matter particle mass M_x.

The prior range set for free parameters are given at Table 4

Table 4. Parameters and priors used in analysis

parameter	initial	prior
$\Omega_{2,0}$	0.3	$\mathcal{U}[0.0, 1.0]$
n	0	$\mathcal{U}[-10, 10]$
$\log_{10}(\kappa C_1/\mathrm{Gyr}^{-1})$	—	$\mathcal{U}[-10, 0]$
$H_0[\mathrm{km/s/Mpc}]$	70	$\mathcal{U}[60, 80]$
β_0	6	$\mathcal{U}[-15, 15]$
β_1	1	$\mathcal{U}[-10, 10]$
γ_0	0.6	$\mathcal{U}[0.0, 1.0]$
γ_1	0	$\mathcal{U}[-1.0, 1.0]$
δ	0.2	$\mathcal{U}[0.0, 1.0]$
$r_{\mathrm{d}}h[\mathrm{Mpc}]$	100	$\mathcal{U}[50, 150]$

4.1. *Model 1: mimicking the ΛCDM model*

The Eq.(8) convergant to the flat ΛCDM model as $\log_{10}(\kappa C_1) \to -\infty$, therefore the constraints could only

give the upper limit of what, and give the lower limit of M_x according to Eq.(9), respectively.

We use the 99% and 1% quantiles to determine the upper and lower limits of the parameters, and the results are shown in Table 5.
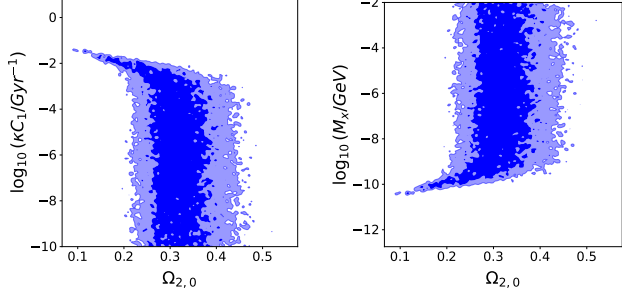

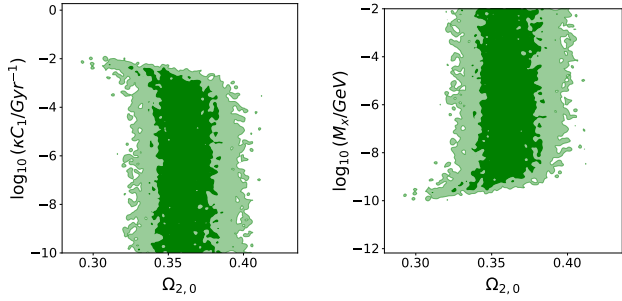**Figure 1.** The constraint result from the observational $H(z)$ data

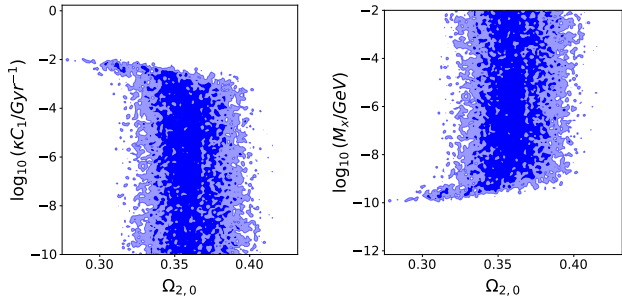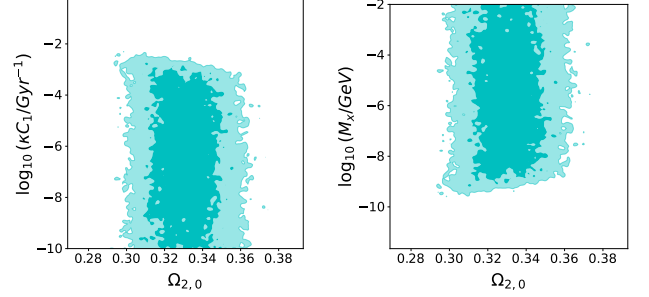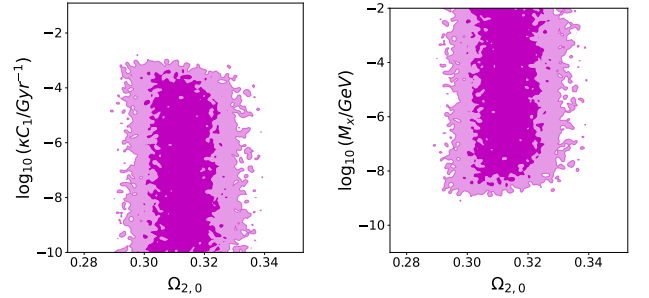**Figure 2.** The constraint result from the supernovae Ia data

Figure 3. The constraint result from the SNe Ia + QSO data

We would find that the SNe Ia and QSO combined result is most similar to SNe Ia result, what may refer that the QSO cannot give an effective constraint.

4.2. *Model 2: mimicking the wCDM model*

The constraint results of Model 2 are shown in Table 6.
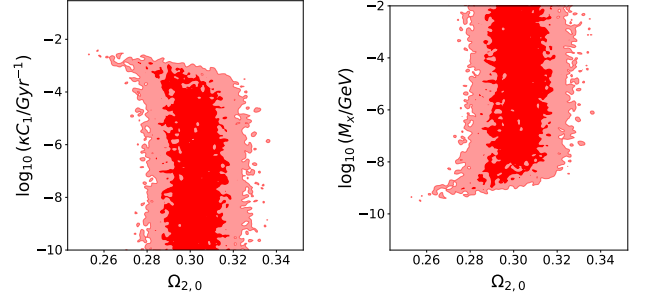
Figure 4. The constraint result from the BAO data

Figure 5. The constraint result from the OHD + SNe Ia data

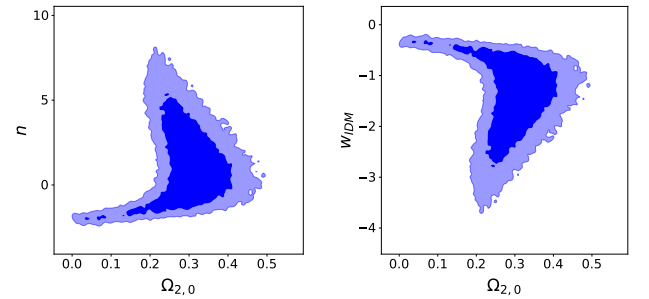**Figure 6.** The constraint result from the OHD + SNe Ia + BAO data
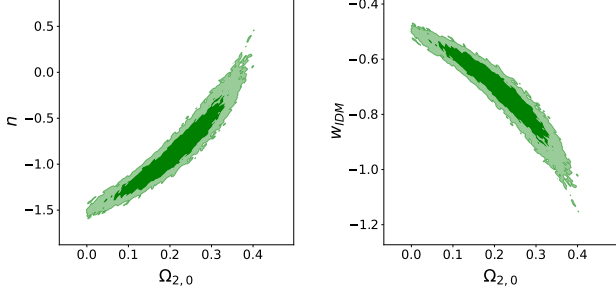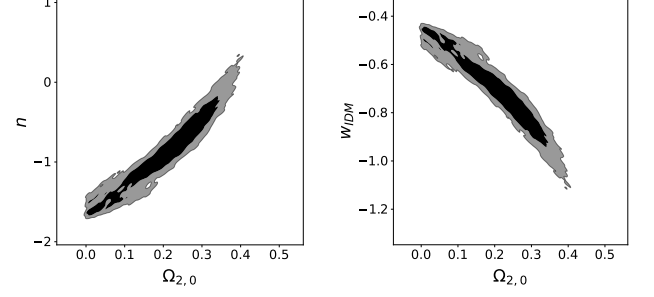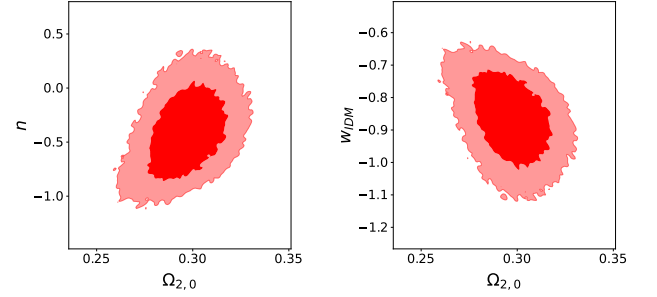

Figure 7. The constraint result from the observational $H(z)$ data

Table 5. The constraint results of Model 1

Model 1	OHD	SNe Ia	SNe Ia + QSO	BAO	OHD + SNe Ia	OHD + SNe Ia + BAO
$\Omega_{2,0}$	$0.321^{+0.055}_{-0.067}$	$0.360^{+0.020}_{-0.020}$	$0.359^{+0.020}_{-0.020}$	$0.301^{+0.013}_{-0.013}$	$0.330^{+0.016}_{-0.016}$	$0.313^{+0.010}_{-0.010}$
$\log_{10}(\kappa C_1/\mathrm{Gyr}^{-1})$	< -1.81	< -2.30	< -2.35	< -2.66	< -2.78	< -3.21
$\log_{10}(M_x/\mathrm{GeV})$	> -10.09	> -9.62	> -9.60	> -9.25	> -9.15	> -8.70

Figure 8. The constraint result from the supernovae Ia data

Figure 9. The constraint result from the SNe Ia + QSO data

Figure 10. The constraint result from the BAO data

The results from three dataset are different

5. CONCLUSIONS

APPENDIX

A. THE THEORETICAL SOLUTION OF MODEL 1

Apply the Eq.(12) to Eq.(8), we can get a simple nonlinear second-order differential equation for the redshift $z(t)$, which can be written as

$$2H_0^2\Omega_{1,0}(1+z)^2z'z'' + \kappa C_1 z'^4 - 5H_0^2\Omega_{1,0}(1+z)z'^3 + 3H_0^4\Omega_{1,0}^2(1+z)^3z' - H_0^4\Omega_{1,0}^2\kappa C_1[(z+1)^4-1] = H_0^4\Omega_{1,0}^2\kappa C_1, \quad \text{(A1)}$$

where the prime denotes the derivative with respect to t. The equation can be simplified as

$$2H_0^2\Omega_{1,0}y^2y'y'' + \kappa C_1 y'^4 - 5H_0^2\Omega_{1,0}yy'^3 + 3H_0^4\Omega_{1,0}^2y^3y' - H_0^4\Omega_{1,0}^2\kappa C_1 y^4 = 0, \quad \text{(A2)}$$

where $y = z+1$, now it is a homogeneous function and we can give the general solution as $y = \exp f$ with f a function of t, the equation now is

$$2H_0^2\Omega_{1,0}f'f'' + \kappa C_1 f'^4 - 3H_0^2\Omega_{1,0}f'^3 + 3H_0^4\Omega_{1,0}^2f' - H_0^4\Omega_{1,0}^2\kappa C_1 = 0. \quad \text{(A3)}$$
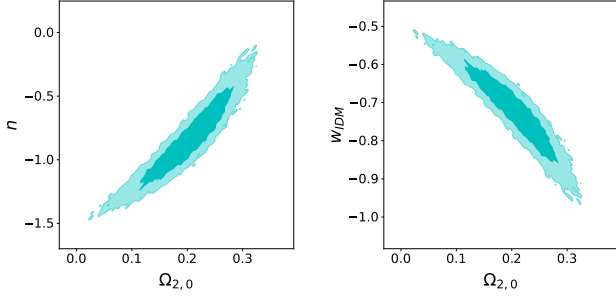
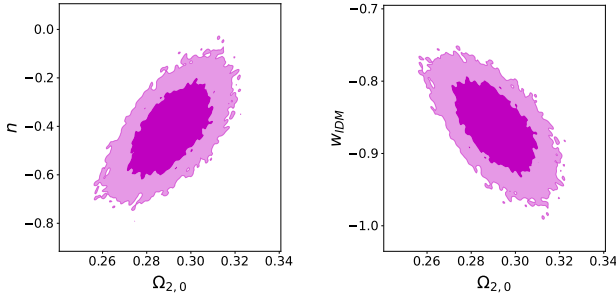**Figure 11.** The constraint result from the OHD + SNe Ia data

Figure 12. The constraint result from the OHD + SNe Ia + BAO data

Table 6. The constraint results of Model 2

Model 2	OHD	SNe Ia	SNe Ia + QSO	BAO	OHD + SNe Ia	OHD + SNe Ia + BAO
$\Omega_{2,0}$	$0.295^{+0.077}_{-0.077}$	$0.216^{+0.096}_{-0.078}$	$0.208^{+0.12}_{-0.087}$	$0.296^{+0.014}_{-0.014}$	$0.202^{+0.060}_{-0.049}$	$0.291^{+0.013}_{-0.013}$
n	$1.4^{+1.4}_{-2.8}$	$-0.82^{+0.29}_{-0.44}$	$-0.85^{+0.42}_{-0.49}$	$-0.40^{+0.29}_{-0.29}$	$-0.83^{+0.24}_{-0.27}$	$-0.41^{+0.13}_{-0.13}$
w_{IDM}	$-1.5^{+0.5}_{-0.9}$	$-0.73^{+0.10}_{-0.15}$	$-0.72^{+0.14}_{-0.16}$	$-0.87^{+0.10}_{-0.10}$	$-0.72^{+0.09}_{-0.09}$	$-0.86^{+0.04}_{-0.04}$

We use $g = f'$, which also gives $g(t) = y'/y = -H(t)$, then the equation can be written as

$$2H_0^2\Omega_{1,0}gg' + \kappa C_1 g^4 - 3H_0^2\Omega_{1,0}g^3 + 3H_0^4\Omega_{1,0}^2 g - H_0^4\Omega_{1,0}^2\kappa C_1 = 0. \tag{A4}$$

It can be theoretically solved and the solution is like

$$g(t) = \mathcal{G}\left(-\frac{t}{2H_0^2\Omega_{1,0}} + Const\right), \tag{A5}$$

where $\mathcal{G}$ is the inverse function of

$$\mathcal{F}(x) = \frac{3H_0\sqrt{\Omega_{1,0}}\operatorname{arctanh}\frac{x}{H_0\sqrt{\Omega_{1,0}}} - \kappa C_1 \log(x^2 - H_0^2\Omega_{1,0}) + \kappa C_1 \log(\kappa C_1 x^2 - 3H_0^2\Omega_{1,0}x + H_0^2\Omega_{1,0}\kappa C_1)}{9H_0^4\Omega_{1,0}^2 - 4H_0^2\Omega_{1,0}(\kappa C_1)^2}. \tag{A6}$$

In this term, $\operatorname{arctanh}(x) \doteq \frac{1}{2}\log\left(\frac{x+1}{x-1}\right)$ when $x < -1$, and the $Const$ is determined by the boundary condition $g(0) \to -\infty$, which is

$$Const = \mathcal{F}(-\infty) \equiv \lim_{x \to -\infty} \mathcal{F}(x) = \frac{\kappa C_1 \ln \kappa C_1}{H_0^2\Omega_{1,0}[-4(\kappa C_1)^2 + 9H_0^2\Omega_{1,0}]}. \tag{A7}$$

The initial time of today t_0 can be easily given as

$$t_0 = 2H_0^2\Omega_{1,0}[\mathcal{F}(-\infty) - \mathcal{F}(-H_0)], \tag{A8}$$

and the redshift z_{max} can be calculated as

$$z_{\mathrm{max}} = \exp\left[\int_{-\infty}^{-H_0} [\mathcal{F}(-\infty) - \mathcal{F}(x)]\mathrm{d}x + \frac{t_0}{2H_0\Omega_{1,0}}\right] - 1, \tag{A9}$$

and z_{max} is also a function of $\Omega_{2,0}, \kappa C_1$ and H_0.
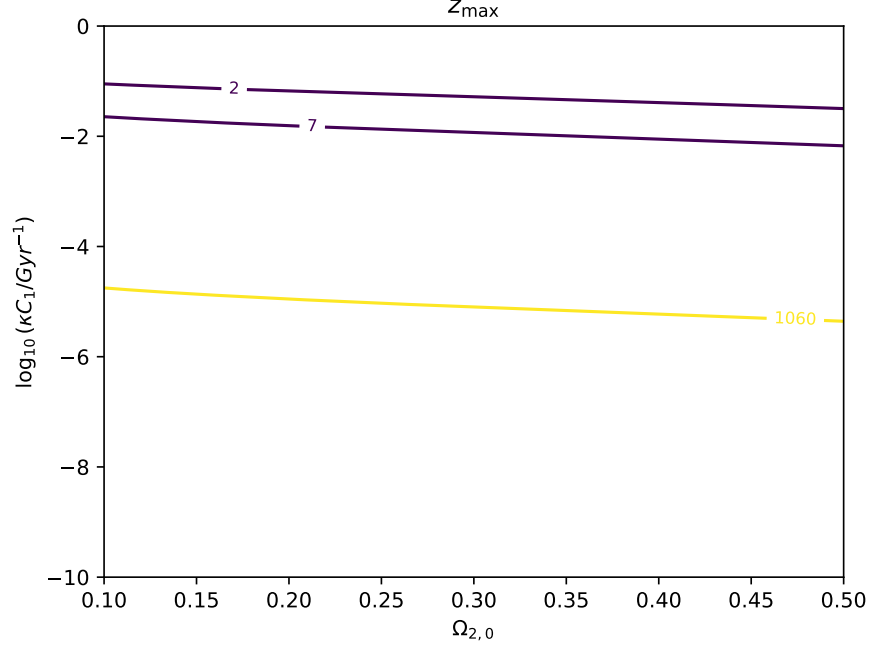

Figure 13. The redshift z_{max} as $H_0 = 70$ km/s/Mpc

REFERENCES

Alam, S., Aubert, M., Avila, S., et al. 2021, Phys. Rev. D, 103, 083533

Basilakos, S., & Plionis, M. 2009, A&A, 507, 47

Borghi, N., Moresco, M., & Cimatti, A. 2022, The Astrophysical Journal Letters, 928, L4

Collaboration, D., Adame, A. G., Aguilar, J., et al. 2024, DESI 2024 VI: Cosmological Constraints from the Measurements of Baryon Acoustic Oscillations. https://arxiv.org/abs/2404.03002

Jiao, K., Borghi, N., Moresco, M., & Zhang, T.-J. 2023, The Astrophysical Journal Supplement Series, 265, 48

Li, X., Keeley, R. E., & Shafieloo, A. 2024, Redshift evolution of the X-ray and UV luminosity relation of quasars: calibrated results from SNe Ia. https://arxiv.org/abs/2408.15547

Lusso, E., Risaliti, G., Nardini, E., et al. 2020, A&A, 642, A150

Moresco, M. 2015, Monthly Notices of the Royal Astronomical Society: Letters, 450, L16

Moresco, M., Cimatti, A., Jimenez, R., et al. 2012, Journal of Cosmology and Astroparticle Physics, 2012, 006

Moresco, M., Pozzetti, L., Cimatti, A., et al. 2016, Journal of Cosmology and Astroparticle Physics, 2016, 014

Ratsimbazafy, A. L., Loubser, S. I., Crawford, S. M., et al. 2017, Monthly Notices of the Royal Astronomical Society, 467, 3239

Riess, A. G., Yuan, W., Macri, L. M., et al. 2022, The Astrophysical Journal Letters, 934, L7

Scolnic, D., Brout, D., Carr, A., et al. 2022, The Astrophysical Journal, 938, 113

Simon, J., Verde, L., & Jimenez, R. 2005, Phys. Rev. D, 71, 123001

Stern, D., Jimenez, R., Verde, L., Kamionkowski, M., & Stanford, S. A. 2010, Journal of Cosmology and Astroparticle Physics, 2010, 008

Zhang, C., Zhang, H., Yuan, S., et al. 2014, Research in Astronomy and Astrophysics, 14, 1221